

Physics and chemistry of hydrogen in the vacancies of semiconductors

Bernadett Szűcs,^{1,2} Adam Gali,¹ Zoltán Hajnal,^{2,3} Peter Deák,¹ and Chris G. Van de Walle⁴

¹*Department of Atomic Physics, Budapest University of Technology and Economics, Budafoki út 8., H-1111, Budapest, Hungary*

²*Theoretische Physik, Universität Paderborn, D-33098 Paderborn, Germany*

³*Research Institute for Technical Physics and Materials Science, P.O.B. 49, Budapest, H-1525 Hungary*

⁴*Palo Alto Research Center, 3333 Coyote Hill Road, Palo Alto, California 94304, USA*

(Received 18 February 2003; published 4 August 2003)

Hydrogen is well known to cause electrical passivation of lattice vacancies in semiconductors. This effect follows from the chemical passivation of the dangling bonds. Recently it was found that H in the carbon vacancy of SiC forms a three-center bond with two silicon neighbors in the vacancy, and gives rise to a new electrically active state. In this paper we examine hydrogen in the anion vacancies of BN, AlN, and GaN. We find that three-center bonding of H is quite common and follows clear trends in terms of the second-neighbor distance in the lattice, the typical (two-center) hydrogen–host-atom bond length, the electronegativity difference between host atoms and hydrogen, as well as the charge state of the vacancy. Three-center bonding limits the number of H atoms a nitrogen vacancy can capture to two, and prevents electric passivation in GaAs as well.

DOI: 10.1103/PhysRevB.68.085202

PACS number(s): 71.15.Mb, 61.72.Bb, 61.72.Ji, 71.55.Eq

I. INTRODUCTION

Hydrogen is known to passivate intrinsic defects but also dopants in many semiconductors. The passivation of defects is both chemical and electrical: hydrogen saturates the dangling bonds and the resulting bonding and antibonding orbitals are removed from the gap. This happens, e.g., in the case of the vacancy in silicon $\text{Si}:V_{\text{Si}}$, (Ref. 1) and the silicon vacancy in silicon carbide $\text{SiC}:V_{\text{Si}}$.² Recently it was found, however, that H in the carbon vacancy in SiC ($\text{SiC}:V_{\text{C}}$) does not follow this trend.³ Instead of forming a normal Si-H bond, it is more favorable for hydrogen to assume a symmetric position between two of the Si atoms surrounding the vacancy. A three-center bond is formed, in which two electrons envelop the three atoms of a (Si-H-Si) bridge. The level corresponding to this three-center bond is below the valence band edge, while the one corresponding to the long bond between the other two silicon atoms is in the lower half of the gap. The electron introduced by the H atom is placed in the antibonding combination of the sp^3 hybrids of its Si neighbors, so that the H atom is at the node of this orbital. As a consequence, the corresponding level lies high in the gap, making the system a hole trap. A second H atom trapped by the vacancy forms another three-center bond with the other two Si neighbors. The system becomes thus a double hole trap. Since capturing further hydrogen atoms is energetically not feasible, no passivation of $\text{SiC}:V_{\text{C}}$ can be achieved. ($\text{SiC}:V_{\text{C}}$ itself is a double hole trap with a level slightly above midgap.)

Gali *et al.* explained the overcoordination of hydrogen in $\text{SiC}:(V_{\text{C}}+\text{H})$ based on geometrical arguments.³ The Si-Si distance across the carbon vacancy in SiC is about 3.1 Å while the normal Si-H bond length is ~ 1.5 Å, so the H atom can interact with two Si atoms. We also note that the second-neighbor distance of bulk SiC is 3.2 Å, which agrees well with the Si-Si distance around a bond-centered interstitial H in crystalline Si. The three-center bond thus requires little atomic relaxation in SiC.

Looking for analogous geometrical relations in other semiconductors (see Table I), we find that in group III nitrides the distance between cations is also comparable to twice the typical cation–hydrogen bond length. Therefore it seems plausible that overcoordination of hydrogen may occur in the nitrogen vacancy ($\text{XN}:V_{\text{N}}$). The main goal of this paper is to predict the trend in the behavior of hydrogen in such cases.

Nitrides of group III elements have tight lattice structures, high melting points, and they are chemically inert and mechanically hard. GaN, due to its large and direct gap, is being successfully used in optoelectronic applications. AlN can be used as an insulator or a barrier layer. $\text{Ga}_x\text{Al}_{1-x}\text{N}$ ternaries are also used as barriers in quantum well structures and as cladding layers. In cubic BN (*c*-BN), EPR measurements have indicated that the nitrogen vacancy is the dominant paramagnetic center.⁴ The prevalence of the nitrogen va-

TABLE I. Geometrical data relevant for H in the vacancies of various semiconductors. The H-C and H-A distances refer to typical bond lengths between hydrogen and a given cation (C) or anion (A) atom species. Overcoordination of hydrogen in the vacancy can be expected if twice the H-C or H-A bond length (Ref. 33) is comparable to the second neighbor (Ref. 34) distance in the corresponding semiconductor.

CA semiconductors	second neighbor distance (Å)	typical H-C distance (Å)	typical H-A distance (Å)
SiC	3.08	1.5	1.1
BN	2.54	1.2	1.0
BP	3.21	1.2	1.4
AlN	3.11	1.6	1.0
GaN	3.16	1.6	1.0
AlAs	4.00	1.6	1.5
GaAs	3.99	1.6	1.5

TABLE II. Summary of structural results for the hydrogenated anion vacancy in different charge states. Information about cation-cation and cation-hydrogen bonds is included to facilitate establishing trends. ΔX is the Pauling electronegativity difference between hydrogen and the cation. $d(\text{bulk})_{cc}$ is the first neighbor distance in the bulk cation crystal, $d(\text{sc})_{cc}$ is the cation-cation distance in the semiconductor, and d_{ch} the normal cation-hydrogen distance.

	BN:(V_N+H) $^{0+q}$	SiC:($V_{Si}+H$) $^{1+q}$	SiC:(V_C+H) $^{1+q}$	GaN:(V_N+H) $^{0+q}$	AlN:(V_N+H) $^{0+q}$
ΔX	+0.1	-0.3	+0.3	+0.5	+0.6
d_{ch} [Å]	1.23	1.11	1.62	1.63	1.64
$d(\text{bulk})_{cc}$ [Å]	1.58	1.54	2.35	2.44	2.86
$d(\text{sc})_{cc}$ [Å]	2.54	3.08	3.08	3.16	3.11
$2 \times d_{ch}/d(\text{sc})_{cc} - 1$	+3%	+31%	+6%	-1%	-6%
$d(\text{sc})_{cc}/d(\text{bulk})_{cc} - 1$	61%	107%	32%	30%	9%
$q = +2$	H on center	not stable	H on center	H on center	H on center
$q = 0$	two center B-H bond	two center C-H bond	inward puckered three-c. Si-H-Si b.	linear three-c. Ga-H-Ga bond	outward puckered three-c. Al-H-Al b.
$q = -2$	inw. puckered three-c. B-H-B b.	two-center C-H bond	not stable	outw. puckered three-c. Ga-H-Ga b.	outw. puckered three-c. Al-H-Al b.

cancy was also shown by near-edge x-ray absorptions fine structure measurements.⁵ Theoretical calculations have shown that nitrogen vacancies have the lowest formation energy among intrinsic point defects.⁶ The electronic structure of the nitrogen vacancy in *c*-BN is still disputed in the literature,⁷⁻¹⁰ but there seems to be agreement that these vacancies are the most abundant point defects in *c*-BN. In hexagonal AlN (*h*-AlN) the nitrogen vacancy was found to be an amphoteric center.¹¹⁻¹³ The importance of vacancies in GaN has been also shown.¹⁴ In *p*-type GaN, the nitrogen vacancy is the most stable intrinsic defect, while in *n*-type GaN, the gallium vacancy is most stable. The nitrogen vacancy in GaN is a shallow donor.

Many growth techniques for group III nitrides introduce hydrogen¹⁵⁻¹⁸ into the growth environment, as in the case of metal-organic chemical vapor deposition (MOCVD) where metal-organic compounds and ammonia are employed as precursors.¹⁹ The established occurrence of V_N defects in these technologically important materials, combined with the

presence of H in the growth process, lends technological importance to our investigations. For purposes of comparison, we have calculated both the bare vacancies ($XN:V_N$) and the $XN:(V_N+H)$ complexes.

The paper is organized as follows. In Sec. II we describe the theoretical methods. Results for XN semiconductors, where $X=B, Al$, or Ga will be given in Secs. III A, III B, III C, respectively, while in Sec. III D we address the likelihood of formation of V_N+H defects relative to V_N . In Sec. IV we discuss the trends in the behavior of hydrogen in group III nitride vacancies. Finally, in Sec. V we summarize our results.

II. METHOD

Our calculations are based on density-functional theory in the local-density approximation (LDA)²⁰ using the Perdew-Zunger exchange-correlation potential.^{21,22} The FHI96MD code²³ was used for plane-wave supercell calculations with a

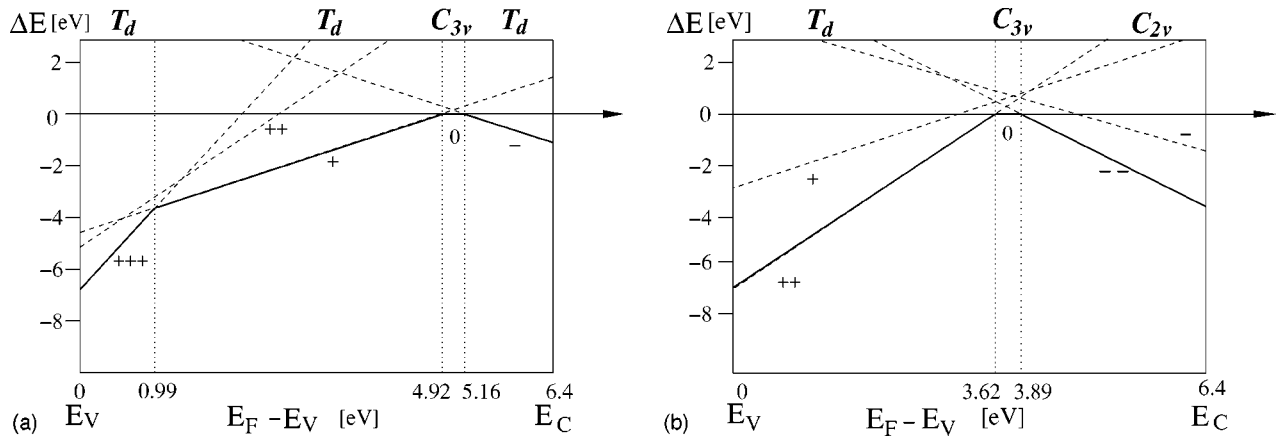


FIG. 1. Relative stability of the different charge states with respect to the neutral one as a function of the Fermi level position for (a) *c*-BN: V_N and (b) *c*-BN:(V_N+H). The symmetry of the lowest-energy configuration is indicated at the top of the diagram.

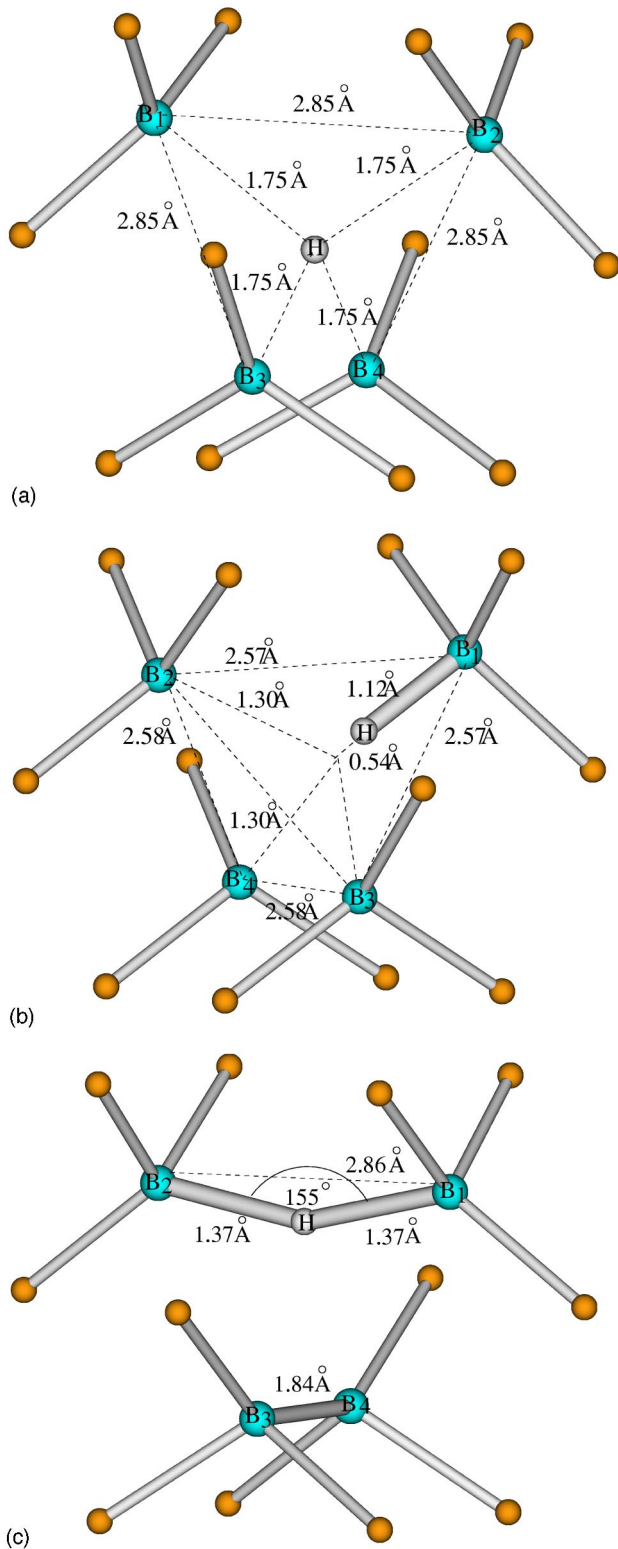


FIG. 2. The geometry of $c\text{-BN}:(V_N+H)$ complex in the (a) $(2+)$, (b) (0) , and (c) $(2-)$ charge states. The small balls represent N atoms connected to B.

64 Ry cutoff in $c\text{-BN}$ and $c\text{-GaN}$ and a 48 Ry cutoff in $h\text{-AlN}$. Troullier-Martins norm conserving soft-core pseudopotentials²⁴ were applied. Cubic BN and GaN were modeled by 32-atom bcc supercells while a hexagonal 72-

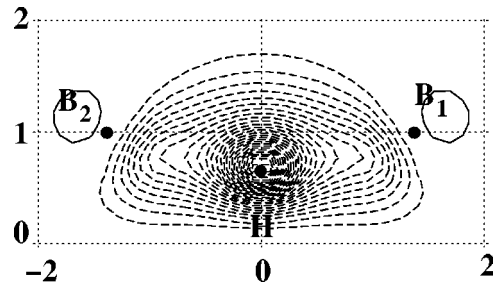


FIG. 3. Example of a three-center bond: B-H-B in the $c\text{-BN}:(V_N+H)^{2-}$ complex. The real part of the corresponding canonical orbital is shown. The coordinates on the axes are in Å.

atom supercell was employed for $h\text{-AlN}$. In each case the Brillouin-zone sampling was performed with a $2 \times 2 \times 2$ Monkhorst-Pack mesh.²⁵ The defect geometry was determined by allowing two shells of host atoms to relax around the defect. The convergence criterion for the forces was 0.0005 Hartree/Bohr.

Density-functional theory is known to underestimate the width of the gap. For extended states in the conduction band, a rigid shift of the energy bands usually suffices to achieve approximate agreement with the experimentally observed excitation energies. Defect orbitals, however, tend to be mixtures of valence-band (VB) and conduction-band (CB) states. No rigorous scheme is currently available for correcting the position of defect states. Here we have used the correction introduced by Baraff and Schlüter,²⁶ which shifts a defect-induced Kohn-Sham state by an amount determined by its degree of conduction band (versus valence-band) character.

Another correction in the position of defect levels (and in the total energy) is made necessary by the dispersion due to the interaction of repeated defects in the supercell. An approximate position of the “isolated” defect level was found by fitting a tight binding dispersion relation to the energies calculated at different \mathbf{k} points. The total energy was corrected by the shift of the one-electron energies. For more details see Ref. 2.

In spite of these corrections the calculated results will still suffer from two kinds of systematic errors. The lack of spin polarization underestimates the stability of spin-half defects by an amount on the order of ≈ 0.1 eV. The lack of charge-state corrections,^{27,32} on the other hand, may overestimate the stability of charged defects by 0.2–0.4 eV.

For BN we studied the cubic zinc blende modification ($c\text{-BN}$), which is the insulating one. GaN is semiconducting in both the zinc blende ($c\text{-GaN}$) and the hexagonal wurtzite ($h\text{-GaN}$) modifications. Since it was shown that the geometry and electronic structure of intrinsic defects are very similar in these two modifications,²⁸ we have carried out our calculations for $c\text{-GaN}$. The lattice constant was optimized and found to be within 1.5% of the experimental values both for $c\text{-BN}$ and for $c\text{-GaN}$. We have used the theoretical lattice constant in the defect calculations. For AlN we have studied the wurtzite $h\text{-AlN}$ modification with lattice constants fixed at the experimental values, but optimizing the atomic positions within the supercell.

Based on earlier experience the approximations that are

TABLE III. The position of the localized one-electron defect levels (Kohn-Sham levels) with respect to the valence-band maximum, and their occupation in different charge states

systems	symmetry	one-electron levels	repr.	occupation
BN:(V _N +H) ²⁺	<i>T_d</i>	-2.8 eV	<i>a</i> ₁	2
		+4.7 eV	<i>t</i> ₂	0
BN:(V _N +H) ⁰	<i>C</i> _{3<i>v</i>}	-2.6 eV	<i>a</i> ₁	2
		+2.9 eV	<i>a</i> ₁	2
		+5.0 eV	<i>e</i>	0
BN:(V _N +H) ²⁻	<i>C</i> _{2<i>v</i>}	-3.8 eV	<i>a</i> ₁	2
		+2.2 eV	<i>a</i> ₁	2
		+4.6 eV	<i>b</i> ₁	2
		+7.3 eV	<i>b</i> ₂	0
		+7.5 eV	<i>a</i> ₁	0
AlN:(V _N +H) ²⁺	<i>C</i> _{3<i>v</i>}	-6.5 eV	<i>a</i> ₁	2
		+4.4 eV	<i>a</i> ₁	0
		+4.7 eV	<i>e</i>	0
AlN:(V _N +H) ⁰	<i>C</i> _{1<i>h</i>} ³⁴	-2.6 eV	<i>a</i> '	2
		+2.4 eV	<i>a</i> '	2
		+4.9 eV	<i>a</i> '	0
		+5.1 eV	<i>a</i> '	0
AlN:(V _N +H) ²⁻	<i>C</i> _{1<i>h</i>} ³⁴	-6.2 eV	<i>a</i> '	2
		+2.3 eV	<i>a</i> '	2
		+4.5 eV	<i>a</i> '	2
		+5.1 eV	<i>a</i> '	0
		+6.5 eV	<i>a</i> ''	0
GaN:(V _N +H) ²⁺	<i>T_d</i>	-7.14 eV	<i>a</i> ₁	2
		+3.76 eV	<i>t</i> ₂	0
GaN:(V _N +H) ⁰	<i>C</i> _{2<i>v</i>}	-7.46 eV	<i>a</i> ₁	2
		+1.55 eV	<i>a</i> ₁	2
		+3.65 eV	<i>b</i> ₁	0
		+4.14 eV	<i>b</i> ₂	0
GaN:(V _N +H) ²⁻	<i>C</i> _{2<i>v</i>}	-7.49 eV	<i>a</i> ₁	2
		+1.28 eV	<i>a</i> ₁	2
		+2.90 eV	<i>b</i> ₁	2
		+3.51 eV	<i>b</i> ₂	0
		+5.67 eV	<i>a</i> ₁	0

pointed out here are acceptable in light of the main goal of our present study, which is to establish qualitative trends rather than predict properties quantitatively. Therefore, no convergence checks were carried out. Occupation levels will be given respect to the perfect crystal valence band edge.

To study the energetics of V_N and V_N+H complexes we calculated their formation energies, based on the following definition:

$$\begin{aligned}
 E_{\text{form}}^q(n_X, n_N, n_H; \mu_X, \mu_N, \mu_H, E_F) \\
 = E_{\text{tot}}^q(n_X, n_N, n_H) - n_X \mu_X - n_N \mu_N - n_H \mu_H + q E_F,
 \end{aligned}
 \tag{1}$$

where n_X denotes the number of X atoms ($X=B, Al, Ga$) and μ_X denotes their chemical potential.^{1,29} E_F is the Fermi energy or chemical potential of the electrons.

In the present study we only investigate differences in formation energy: either between different charge states of the same defect, or between the bare and the hydrogenated vacancy. In the former case the explicit knowledge of the chemical potentials is not required, while only μ_H is needed in the latter:

$$\Delta E_{\text{form}} = E_{\text{tot}}^{q_1}(V_N) - E_{\text{tot}}^{q_2}(V_N+H) + \mu_H + (q_1 - q_2) E_F.
 \tag{2}$$

The sign has been chosen such that ΔE_{form} is positive when the hydrogenated vacancy is more stable than the bare vacancy. For μ_H we will use the energy of hydrogen in the H_2 molecule at 0 K as a reference. The $3d$ electrons of Ga were treated as part of the ionic core. In the only case where explicit formation energy is quoted, nonlinear core correction is used.

III. RESULTS

A. Cubic boron nitride

In c -BN the neutral nitrogen vacancy without relaxation is, in principle, Jahn-Teller unstable since three electrons occupy an a_1 and a t_2 state. The lowest energy configuration has C_{3v} symmetry. The B-B distances increased on average by 4% and the difference between them is just about 1%. Two defect levels arise in the band gap corresponding to a doubly occupied a_1 state at about $E_v + 0.1$ eV and to a singly occupied a_1 state at about $E_v + 5.1$ eV. The calculated energy difference between the T_d and C_{3v} configurations is only 6 meV. The small Jahn-Teller distortion and the outward relaxation of the boron atoms is understandable since the boron-boron distances across the vacancy are much longer than the B-B distance in a bulk boron crystal (see Table II). Consequently the bonds between the boron atoms are weak and do not compensate the attraction of the nitrogen neighbors. The situation here is similar to that of the silicon vacancy in SiC.³

We also calculated the (3+), (2+), (1+), and (-1) charge states of the boron vacancy. Figure 1(a) summarizes the relative stabilities as a function of the Fermi level position in the gap (which can be changed by extrinsic doping). The (2+) charge state is not stable for any Fermi level position. The vacancy has negative- U character and could be an electron as well as a hole trap (as it is the case for SiC: V_C^-). The negative charge state, c -BN: V_N^- can be directly compared to SiC: V_{Si}^0 both having four electrons. In the unrelaxed c -BN: V_N^- , two electrons are on the t_2 state which makes it still Jahn-Teller unstable, however, the geometry does not change substantially upon relaxation. The boron atoms relaxed outward by 0.6% and the T_d symmetry is almost conserved (as happens in SiC: V_{Si}^0).

Hydrogen in the nitrogen vacancy, c -BN:(V_N+H^0), in the neutral charge state, simply gives rise to a single boron-hydrogen bond, and the defect has C_{3v} geometry (see Fig. 2). Comparing the minimum-energy configuration of the different charge states [see Fig. 1(b)], we found that only the

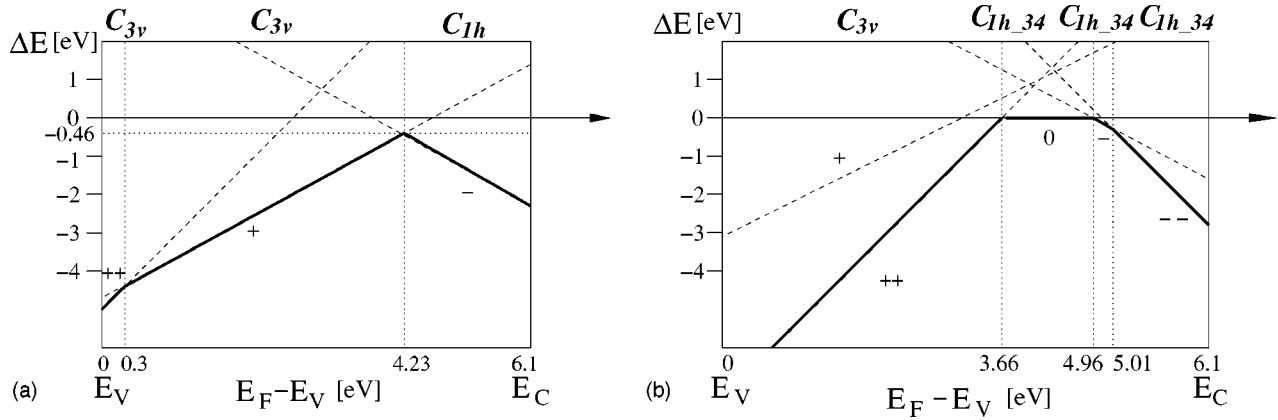


FIG. 4. Relative stability of the different charge states with respect to the neutral one as a function of the Fermi level position for (a) $h\text{-AlN}:V_N$ and (b) $h\text{-AlN}:(V_N+H)$. The symmetry of the lowest-energy configuration is indicated at the top of the diagram.

(2+), (0), and the (2−) charge states are stable (indicative of a negative- U center). In the case of the (2+) charge state hydrogen remains in an on-center position. A doubly occupied a_1 state in the valence band is localized mainly on the hydrogen. No occupied Kohn-Sham levels appear in the band gap. In the (2−) charge state a three-center B–H–B bond appears and the symmetry changes to C_{2v} (see Fig. 2). The energy level corresponding to the three-center bonding orbital is below the valence band edge (see Fig. 3). Two doubly occupied defect levels appear in the band gap. The lower lying state is localized mostly on the hydrogen and on the two boron neighbors that are not part of the B–H–B bond (B_3 – B_4 in Fig. 2). The highest occupied level comes from the antibonding combination of the sp^3 hybrids of the hydrogen's neighbors, so the hydrogen atom is at the node of this orbital. Figure 2 shows the geometry of the V_N+H defect complex in the (2+), (0), and (2−) charge states. The positions of the one-electron levels are summarized in Table III.

B. Hexagonal aluminum nitride

Calculating the nitrogen vacancy in different charge states in $h\text{-AlN}$, we found that it is not stable in the neutral charge state [see Fig. 4(a)]. In the (−1) charge state the aluminum atoms move towards each other in pairs and form two long bonds. In the (1+) charge state the atoms move away from each other, and the system remains almost C_{3v} .

The $h\text{-AlN}:(V_N+H)$ complex in the neutral charge state produces an equilibrium geometry that is surprising at first sight. The hydrogen atom leaves the vacancy and an outward puckered three-center bond is formed with C_{1h} symmetry (Fig. 5). Note that in the hexagonal lattice there are two possible configurations with C_{1h} symmetry, with the hydrogen occupying inequivalent sites. We find hydrogen between Al_3 and Al_4 in Fig. 5 to be more stable than between Al_1 and Al_2 .

We have calculated the relative stabilities of different charge states as a function of the Fermi level position [see Fig. 4(b)]. Apart from a very small window for the Fermi level where the (1−) state is stable, the (2+), (0), or (2−) charge states are the relevant ones. In the case of the (2+)

charge state the hydrogen remains on center with C_{3v} symmetry. In the (2−) charge state the outward puckered Al_3 –H– Al_4 three-center bond is formed, similar to the neutral charge state. Figure 5 displays the geometry of the V_N+H defect in AlN in different charge states. The one-electron levels are given in Table III.

C. Cubic gallium nitride

The vacancy in GaN has been previously investigated.³⁰ Our results regarding the relative stability of different charge states [see Fig. 6(a)] agree qualitatively with the earlier findings, except for small quantitative differences due to the use of different pseudopotentials and due to the gap and dispersion corrections applied in the present study. The previous work reported that the nitrogen vacancy is only stable in the (+) and (3+) charge states. The stability of the negative charge state for a small range of Fermi levels near the conduction band in Fig. 6 is probably an artifact, related to the approximate nature of the corrections that are applied here. In the negative charge state a pairing distortion of cations occurs, similar to AlN. For most Fermi-level positions V_N^+ is stable, while V_N^{2+} is never (negative- U).

The $(V_N+H)^{2+}$ complex was also previously investigated.³⁰ Here we confirm that H is located at the center of the vacancy in this charge state. Our current calculations show that in the neutral charge state hydrogen forms a slightly inward-puckered three-center Ga–H–Ga bond. The energy of this configuration is about 1.3 eV lower than in the high-symmetry configuration where H sits at the center of the vacancy. The three-center-bond configuration generates one doubly-occupied defect level in the band gap corresponding to the long bond between the two Ga atoms not bonded to H. The bonding state of the three-center bond is below the valence band edge. We find the (2−) charge state, with a slightly outward-puckered three-center bond, to be stable in a small range of Fermi levels near the conduction band (subject to the uncertainties in defect levels). The two extra electrons go into an antibonding combination of the orbitals of the two Ga atoms next to the hydrogen. Figures 6(b) and 7 show the relative stability and geometry, respec-

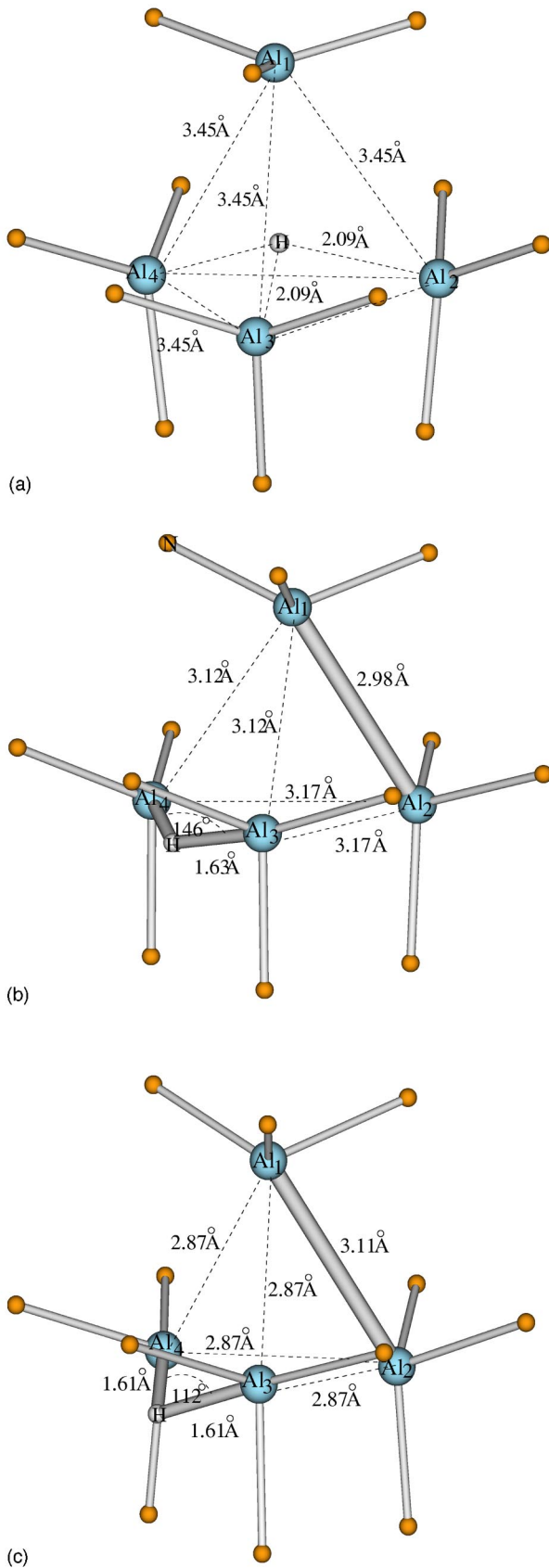


FIG. 5. The geometry of the h -AlN: (V_N+H) defect in the (a) $(2+)$, (b) (0) and (c) $(2-)$ charge states. The small balls represent N atoms connected to Al.

tively, of the V_N+H defect in different charge states in c -GaN; defect levels are summarized in Table III.

We have also investigated the capture of a second and a third hydrogen by the nitrogen vacancy in c -GaN. The second hydrogen forms another three-center bond with the other two Ga neighbors of V_N (similarly to the case of SiC: V_C), and the complex is still electrically active. Three hydrogen atoms in the vacancy form three equivalent two-center bonds but the energy of this complex is higher than that of V_N+2H and an isolated interstitial hydrogen for any Fermi-level position below $E_F-E_V=2.2$ eV, i.e., in the whole doping range where V_N+H defects can be expected. Therefore, the nitrogen vacancy cannot be passivated by hydrogen either. This appears to be a general consequence of the three-center bonding of hydrogen.

D. Stability of the $V+H$ defects in group III nitrides

To examine the stability of the hydrogenated vacancy, let us focus on GaN, which is currently the most widely used among the materials studied here. However, our conclusions for GaN largely apply to AlN and BN as well. We can see from Fig. 6 that nitrogen vacancies are most stable when the Fermi level is in the lower part of the band gap, i.e., under intrinsic or p -type conditions. The same applies to the hydrogenated vacancies. Over most of the relevant range of Fermi levels, the important charge states are $(+)$ and $(3+)$ for V_N , and $(2+)$ for V_N+H . The stability of these charge states was already addressed in Ref. 30. In addition, we now need to consider the neutral charge state of V_N+H . This charge state is the stable one when the Fermi level is more than 2.53 eV above E_V . The formation energy calculated under identical conditions as in Ref. 30 (using nonlinear core correction for Ga, but no correction for the gap and dispersion error) is 3.53 eV. This rather high formation energy makes it unlikely that this defect be created in large concentrations during growth. (Post-growth introduction of hydrogen—for instance via implantation or diffusion—into material that already contains nitrogen vacancies is also unlikely to result in the formation of neutral V_N+H complexes either, because V_N and interstitial hydrogen do not attract each other.) We note that the formation energy of $(V_N+H)^0$ is even larger in AlN and BN, making it even less likely that these defects would form in the neutral charge state under thermal equilibrium conditions.

We do note, however, that the formation energies of $(V_N+H)^{2+}$ are quite low when the Fermi level is low in the gap; lower, in fact, than the formation energy of the bare vacancy. Table IV shows the energy difference between the bare V_N and the V_N+H defects according to Eq. (2) for the Fermi level at midgap (where the former is singly and the latter doubly positive in all three materials). The relative stability of V_N with respect to V_N+H increases as the Fermi energy is lowered (up to the point where V_N becomes triply positive, and the difference starts to decrease again). It is therefore quite likely that large concentrations of these defects are formed under p -type conditions. Some of these hydrogenated vacancies may lose their hydrogen after the sample is grown, during cooldown or during post-growth annealing; this issue

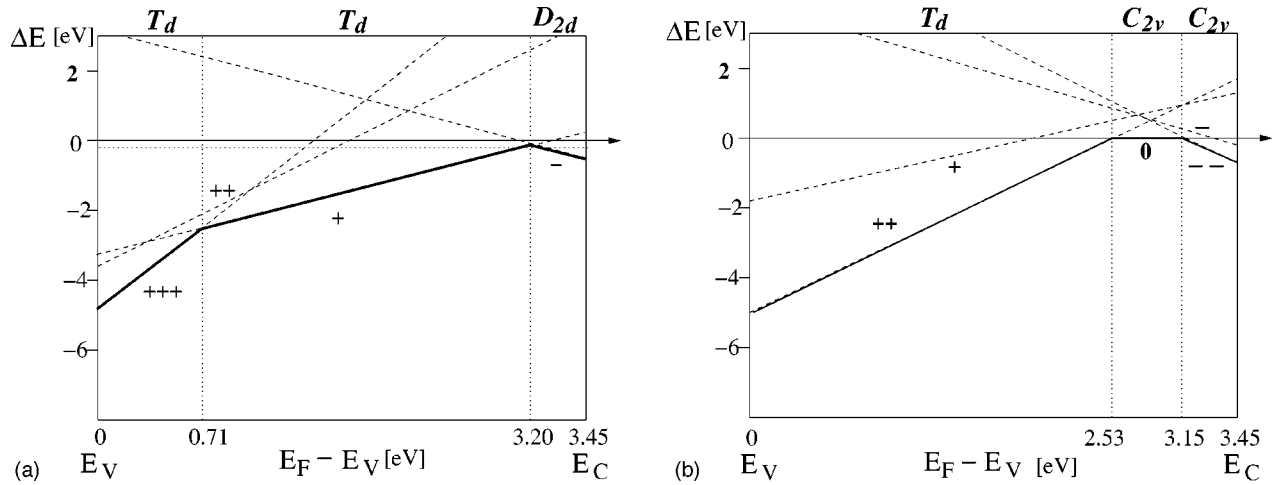


FIG. 6. Relative stability of the different charge states with respect to the neutral one as a function of the Fermi level position for (a) $c\text{-GaN}:V_N$ and (b) $c\text{-GaN}:(V_N+H)$. The symmetry of the lowest-energy configuration is indicated at the top of the diagram.

was addressed for GaN in Ref. 30. For those centers that remain hydrogenated, one may wonder whether the presence of charge states other than $(2+)$, and the ensuing presence of transition levels in the band gap, plays any role in the properties of the material, in particular in photoluminescence. Considering the large relaxations, which are very different between different charge states, an evaluation of transitions that could be observed in photoluminescence requires constructing a configuration coordinate diagram. Such an effort was beyond the scope of the present paper, but preliminary inspection of the results indicates that hydrogenated vacancies in GaN may indeed give rise to various luminescence lines ranging from the red to the blue region of the spectrum.

IV. TRENDS IN THE BEHAVIOR OF HYDROGENATED VACANCIES

We now investigate the electronic structure of the configurations described above in terms of a simple tight binding picture, based on the four cationic sp^3 hybrid orbitals (h_1, \dots, h_4) pointing to the vacancy and the hydrogen's s orbital. In cubic crystals the three-center bonded configuration corresponds to C_{2v} symmetry, which is lowered to C_{1h} in hexagonal crystals. We will concentrate on the former case. In C_{2v} symmetry three a_1 states arise from the linear combination of s , h_1+h_2 and h_3+h_4 . In addition there are the b_1 state of h_1-h_2 and the b_2 state of h_3-h_4 . (In C_{1h} symmetry there are four a' states coming from s , h_1+h_2 and h_3+h_4 and two a'' states corresponding to h_3 and h_4 .) It is convenient to construct the electronic structure of the $V+H$ defect molecule if we start from the reconstructed neutral anion vacancy V_C^0 in SiC and the negative vacancy V_N^- in the nitrides.³¹ The relevant orbitals are shown in Fig. 8, along with the s orbital of the hydrogen.

In order to understand the formation of the three-center bond, we have to start with the vacancy part. We find that the type of relaxation (reconstruction) in the vacancy is crucial. The decisive question is how the cation-cation distance

across the anion vacancy relates to the ideal bonding distance between the cations (see Table II). If the former is much bigger than the latter, then the dangling bonds of the vacancy “retract” and the cations relax outwards. Putting the hydrogen into the vacancy pulls one cation back and gives rise to a normal cation-hydrogen bond. This happens in $\text{SiC}:V_{\text{Si}}$ and in $\text{BN}:V_N$. If the two distances are comparable, however, then a pairing distortion occurs in the vacancy and long bonds will be formed between pairs of the cations. This is the condition for H to form a three-center bond. This happens in $\text{SiC}:V_C$, $\text{AlN}:V_N^-$ and $\text{GaN}:V_N^-$. The situation is depicted in Fig. 8(b) using a defect molecule diagram and assuming cubic crystals (apart from small symmetry differences the situation is the same in the hexagonal lattices of AlN and GaN as well). In the actual calculations the orbitals shown here were identified in all cases by mapping the real part of the one-electron state in the appropriate plane. The positions of defect levels relative to the band edges in Fig. 8 are only schematic.

The essential point is that H^+ “slips into” the long bond between one of the cation pairs (if there exist any), forming a three-center bond and lowering the symmetry from D_{2d} to C_{2v} (in cubic crystals). Quantitative differences arise due to the electronegativity difference (ΔX) between the H and the cations, as well as due to the relation of the ideal cation-cation distance to the cation-cation distance in the semiconductor (see Table II). In the case of $\text{SiC}:V_C$, ΔX is small. The two electrons are evenly distributed over the three centers and H^+ is not well screened. Therefore it is attracted by the electrons of the other cation pair and moves toward the center, forming an inward puckered three-center bond. In the case of GaN, ΔX is bigger, therefore H^+ gets a higher share of the two electrons in the three-center bond, which becomes somewhat ionic making H a strong link in the almost straight Ga–H–Ga bridge. In the case of AlN, ΔX is the largest. H^+ gets most of the two electrons in the three-center bond. Since the other long bond is also well concentrated into the vacancy (the Al–Al distance across the unrelaxed vacancy is

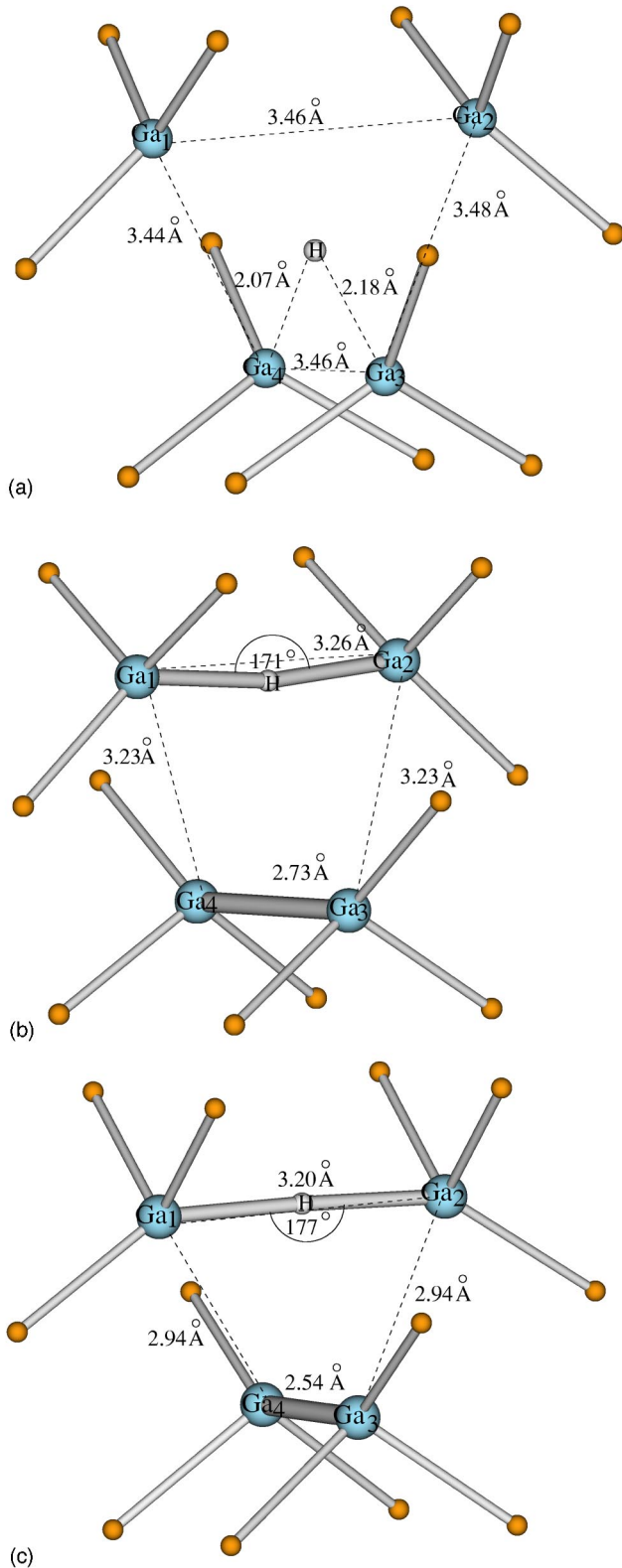


FIG. 7. The geometry of the c -GaN: (V_N+H) defect in the (a) $(2+)$, (b) (0) and (c) $(2-)$ charge states. The small balls represents N atoms connected to Ga.

TABLE IV. Energy of the bare V_N vacancy relative to the V_N+H complex in group III nitrides at 0 K based on Eq. (2) [$\mu_H(H_2) = -15.27$ eV].

	c -BN	h -AlN	c -GaN
ΔE_{form} [eV]	+2.42	+2.30	+1.79

closest to the ideal cation-cation distance), the repulsion between the electrons in that bond and those around H^+ becomes strong: therefore, the Al–H–Al bridge is puckered outwards.

Still, the positive charge of the proton is not completely screened in either case. Therefore, putting one or two electrons into the antibonding combination of the hybrids of the neighboring cations does not destabilize the three-center bond. The increased electron density in the higher negative charge states establishes the bonding configurations described here even in c -BN. The electrostatic interaction makes H pucker outward also in GaN.

Starting from neutral $(V_N+H)^0$ in the nitrides and positive $(V_C+H)^+$ in SiC, it is easy to understand the states with two electrons less (these systems show negative U behavior, so the intermediate charge state is not stable). The situation for the $(2+)$ charge state of the nitrides [$(3+)$ for SiC] can be understood in the scheme of Fig. 8(a). Taking a positive V_N (or doubly positive V_C in SiC) we have an “electron-poor” vacancy, stable in T_d symmetry (assuming cubic crystals). Therefore there is no distinct long bond between the pairs across the vacancy: the four cations share two electrons on a totally symmetric a_1 orbital. In this situation the s -orbital of the on-center H^+ simply interacts with this a_1 state and the T_d symmetry remains.

V. SUMMARY

We have found that the behavior of hydrogen in the anion vacancy in compound semiconductors depends on two key parameters: (1) the ratio of the second-neighbor distance in the semiconductor to the ideal bonding distance between the cations and (2) the ratio of the former to the ideal bonding distance between hydrogen and the cation. If the cation-cation distance in one semiconductor is comparable to twice the cation-hydrogen distance, the necessary condition for forming a three-center bond is established. If the ideal bonding distance between the cations is much less than the second-neighbor distance in the semiconductor then the cations will relax outward and the hydrogen will form a two-center bond with one of them. The sufficient condition for the three-center bond is that the second-neighbor distance in the semiconductor be close to the ideal cation-cation bond length. The geometry of the X–H–X bridge depends on the difference in the electronegativities. Formation of two X–H–X bridges seems to prevent trapping of further hydrogen atoms in the vacancy which, therefore, remains electrically active upon hydrogenation.

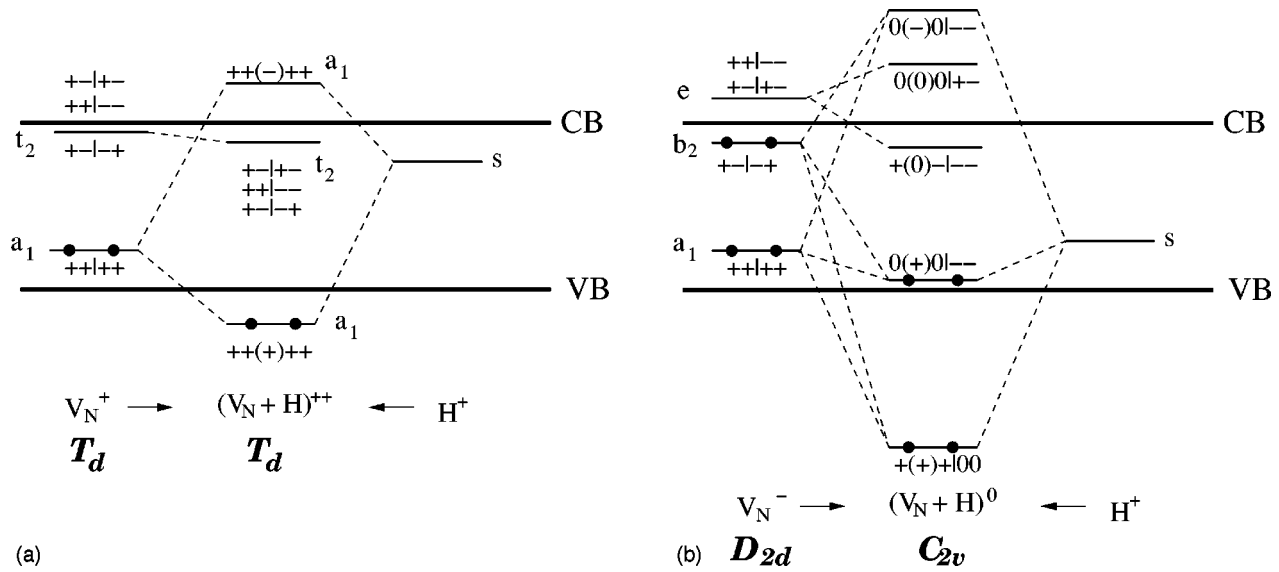


FIG. 8. Defect molecule diagram for $\text{SiC}:(V_C+H)^{3+}$ and for $\text{XN}:(V_N+H)^{2+}$ (a), as well as for $\text{SiC}:(V_C+H)^{1+}$ and $\text{XN}:(V_N+H)^0$ (b), where $X=\text{Al,Ga}$. The signs of the coefficients of the cationic sp^3 -hybrids on both sides of H and that of the s -orbital of H (in parentheses) are given on the left side of the “|” mark, while the signs of the contributions of the other two cations are given on the right side. The second diagram applies also in the case of $\text{XN}:(V_N+H)^{-2}$, but the third defect level will then be doubly occupied.

ACKNOWLEDGMENTS

We wish to thank Professor Thomas Frauenheim at Paderborn University for providing us with additional computational capacities. This work was also supported by the

Hungarian Grant No. OTKA T32174, by the German-Hungarian Grant No. DFG/MTA project No. 112, and by the Air Force Office of Scientific Research, Contract No. F4920-00-C-0019, monitored by G. Witt.

- ¹C. G. Van de Walle, Phys. Rev. B **49**, 4579 (1994).
- ²B. Aradi, A. Gali, P. Deák, J. E. Lowther, N. T. Son, E. Janzén, and W. J. Choyke, Phys. Rev. B **63**, 245202 (2001).
- ³A. Gali, B. Aradi, P. Deák, W. J. Choyke, and N. T. Son, Phys. Rev. Lett. **84**, 4926 (2000).
- ⁴M. Fanciulli and T. D. Moustakas, Physica B **185**, 228 (1993).
- ⁵I. Jiménez, A. F. Jankowski, L. J. Terminello, D. G. J. Sutherland, J. A. Carlisle, G. L. Doll, W. M. Tong, D. K. Shuh, and F. J. Himpsel, Phys. Rev. B **55**, 12 025 (1997).
- ⁶W. Orellana and H. Chacham, Appl. Phys. Lett. **74**, 2984 (1999).
- ⁷P. Piquini, R. Mota, T. M. Schmidt, and A. Fazzio, Phys. Rev. B **56**, 3556 (1997).
- ⁸V. A. Gubanov, Z. W. Lu, B. M. Klein, and C. Y. Fong, Phys. Rev. B **53**, 4377 (1996).
- ⁹I. Gorczyca, A. Svane, and N. E. Christensen, Phys. Rev. B **60**, 8147 (1997).
- ¹⁰W. Orellana and H. Chacham, Phys. Rev. B **62**, 10 135 (2000).
- ¹¹C. Stampfl and C. G. Van de Walle, Appl. Phys. Lett. **72**, 459 (1998).
- ¹²T. Mattila and R. M. Nieminen, Phys. Rev. B **55**, 9571 (1997).
- ¹³A. Fara, F. Bernardi, and V. Fiorentini, J. Appl. Phys. **85**, 2001 (1999).
- ¹⁴J. Neugebauer and C. G. Van de Walle, Phys. Rev. B **50**, 8067 (1994).
- ¹⁵M. Yeadon, M. T. Marshall, S. Pekin, H. Morkoç, and J. M. Gibson, J. Appl. Phys. **83**, 2847 (1998).
- ¹⁶J.N. Russell, Jr., V. M. Bermudez, and A. Leming, J. Vac. Sci. Technol. A **14**, 908 (1996).
- ¹⁷H.-U. Baier and W. Mönch, J. Vac. Sci. Technol. B **10**, 1735 (1992).
- ¹⁸J. Lu, L. Haworth, D. I. Westwood, and J. E. Macdonald, Appl. Phys. Lett. **78**, 1080 (2001).
- ¹⁹L. J. Schowalter, Y. Shusterman, R. Wang, I. Bhat, G. Arunmozhi, and G.A. Slack, Appl. Phys. Lett. **76**, 985 (2000).
- ²⁰W. Kohn and L. J. Sham, Phys. Rev. **140**, A1133 (1965).
- ²¹J. P. Perdew and A. Zunger, Phys. Rev. B **23**, 5048 (1981).
- ²²D. M. Ceperley and B. J. Alder, Phys. Rev. Lett. **45**, 566 (1980).
- ²³M. Bockstedte, A. Kley, J. Neugebauer, and M. Scheffler, Comput. Phys. Commun. **107**, 187 (1997).
- ²⁴N. Troullier and J. L. Martins, Phys. Rev. B **43**, 9393 (1991).
- ²⁵H. J. Monkhorst and J. K. Pack, Phys. Rev. B **13**, 5188 (1976).
- ²⁶G. A. Baraff and M. Schlüter, Phys. Rev. B **30**, 1853 (1984).
- ²⁷Our experience with similar-size supercells indicates that the use of the jellium charge compensation causes an error of about 0.2 eV in case of singly charged systems. In our opinion the monopole term of the frequently applied Makov-Payne (Ref. 32) correction amounts to an overcorrection. Since a rigorous correction for charge-state effects is not yet available, we have refrained from applying any correction.
- ²⁸J. Neugebauer and C. G. Van de Walle, in *Diamond SiC and Nitride Wide-Bandgap Semiconductors*, edited by C.H. Carter,

- Jr., G. Gildeblat, S. Nakamura, and R.J. Nemanich, MRS Symposia Proceedings No. **339** (Materials Research Society, Warrendale, PA, 1994), p. 687.
- ²⁹A. Zywietz, J. Furthmüller, and F. Bechstedt, Phys. Rev. B **59**, 15 166 (1999).
- ³⁰C. G. Van de Walle, Phys. Rev. B **56**, 10 020 (1997).
- ³¹Although V_N^- is not necessarily thermodynamically stable, it forms a convenient starting point for discussing the formation of bonds with hydrogen, resulting in $(V_N+H)^0$. V_N^- has four electrons, and thereby the possibility of forming two equivalent long bonds across the vacancy.
- ³²G. Makov and M.C. Payne, Phys. Rev. B **51**, 4014 (1995).
- ³³*Tables of Interatomic Distances and Configuration in Molecules and Ions*, edited by L. E. Sutton (The Chemical Society, London, 1958).
- ³⁴*Group IV-elements and III-V-compounds, Data in Science and Technology*, edited by O. Madelung (Springer-Verlag, Berlin, 1991).